JOURNAL OF MATERIALS SCIENCE **36** (2001) 2633 – 2638

Nickel nanoparticles inserted in tBuONa matrix deposited on alumina

Part II *Thermal treatment and nickel content effects on their stabilty and catalytitic activity*

S. LEFONDEUR, S. MONTEVERDI, S. MOLINA, M. M. BETTAHAR
Laboratoire de Catalyse Hétérogène, UMR CNRS 7565, Faculté des Sciences, Université Henri Poincaré, BP 239, 54506 Vandœuvre Cedex, France
E-mail: bettahar@lcah.u-nancy.fr

Y. FORT
Laboratoire de Synthèse Organique et Réactivité, UMR CNRS 7565, Faculté des Sciences, Université Henri Poincaré, BP 239, 54506 Vandœuvre Cedex

E. A. ZHILINSKAYA, A. ABOUKAIS
Laboratoire de Catalyse et Environnement, EA 2598, MREID, Université du Littoral Côte d'Opale, 145, Av. Maurice Schumann, 59140 Dunkerque Cedex, France

M. LELAURAIN
Laboratoire de Chimie du Solide Minéral, UMR CNRS 7555, Faculté des Sciences, Université Henri Poincaré, BP 239, 54506 Vandœuvre Cedex, France

Nanoparticles (1 nm–3 nm) of metallic nickel supported on alumina (4.3% Ni–17.9% Ni w/w) were prepared from a colloidal precursor inserted in an organic matrix. Their structural and stability properties have been studied by X-Ray Diffraction (XRD), Electron Paramagnetic Resonance (EPR) and Thermal Gravimetric Analysis (TGA). Benzene hydrogenation at atmospheric pressure in the temperature range of 75 °C–200 °C was used as a test reaction of their catalytic capability. The thermal stability of the particles depended on the nature of the reactive atmosphere. Thus, a growth in size (up to around 20 nm) is observed under H_2 flow at 350 °C or during benzene hydrogenation but not under air flow at 300 °C. The growth may be due to the coalescence of the metal particles during the heating and decomposition of the stabilizing organic matrix. Under oxidative atmosphere, stable nickel oxide particles, firmly attached to the support, are formed. The catalysts pre-treated under H_2/350 °C were active and stable in benzene hydrogenation. The observed activities depended on the reaction conditions and nickel composition.

1. Introduction

The potential applications of nanoparticle powders and films in both industrial and academic fields [1–9] have led to a growing interest in the chemical methods of their preparation [10–24] because of the need of better structure control at the microscopic level. In a previous paper [25] we reported a study on the structural and chemical properties of nanoparticles of metallic nickel previously inserted in an organic matrix (denoted as a NiRC complex) [21–24] supported on γ-alumina. The results obtained showed that, in the supported material (denoted as a NiRCS complex), the metallic nickel phase was well dispersed on the support (1–3 nm) and part of the organic matrix was still present [25]. These materials exhibited molecular hydrogen reservoir properties and were active in the hydrogenation of styrene or benzene in liquid or gas phase media after thermal treatment [25]. The thermal treatment allowed the decomposition of the remaining organic matrix which inhibited the access of the reactant molecules to the nickel phase [25]. In the present paper we report results on the effect of thermal pre-treatment and nickel loading on (i) the stability of the nickel particles and (ii) their catalytic properties in the gas phase hydrogenation of benzene. The structural and chemical properties were investigated by X-Ray Diffraction (XRD), Electron Paramagnetic Resonance (EPR) and Thermal Gravimetric Analysis (TGA). The EPR experiments gave, in addition, supplementary information on the structure of both supported and unsupported nickel particles.

2. Experimental

2.1. Catalyst peparation

The overall procedure of preparation of the nickel materials was previously described [25]. The nickel

composition was varied in the range of about 5% to 20%. All the materials prepared were stored under argon atmosphere. For freshly stored catalysts, practically no atmospheric oxidation of the metallic phase was observed as showed EPR studies: the spectrum of a sample in contact with air for a few minutes was found almost unchanged after 2 months of storage. Oxidation was observed for samples exposed to air for longer times. On the other hand, the NiRC and NiRCS complexes were sensitive to atmospheric moisture as a result of the strong base character of the tBuONa component (see Results and Discussion).

2.2. Catalyst characterization

XRD and TGA experiments were previously described [25]. As to the nickel composition of the catalysts it was determined using a Varian AA1275 atomic absorption spectrophotometer. The EPR measurements were performed at −196 °C and 20 °C on a Bruker EMX spectrometer. A cavity operating at a frequency of 9.5 GHz (X-band) was used. The magnetic field was modulated at 100 kHz. The *g* values were determined from precise frequency and magnetic field values.

2.3. Catalyst testings

The catalyst testing procedure for the gas phase hydrogenation of benzene was previously reported [25]. The present tests were carried out with 0.1 g–0.2 g of catalyst at atmospheric pressure in the temperature and total rate flow ranges of 75 °C–200 °C and 50 $cm^3 \cdot min^{-1}$–130 $cm^3 \cdot min^{-1}$ respectively. In such conditions the reaction was under chemical process control.

3. Results and discussion

3.1. XRD experiments

The metal phase stability as a function of the nickel content under various atmospheres was studied by XRD. The catalysts exhibited the characteristic bands of a metallic nickel phase of classical cfc structure as shown in Fig. 1. As to the metal particle size, as estimated using the Debye-Sherrer equation, it changed as a function of the working conditions as shown in Table I for the C10EW and C11EW catalysts.

The fresh catalyst exhibited a large main band at $2\theta = 44.5°$ (Fig. 1a), attributed to nickel nanophase (1 nm–3 nm), in good accordance with previous studies [25, 26]. After treatment at 300 °C in air the nickel phase

TABLE I Particle size as determined by XRD

Catalyst %Ni		C11 EW 7.6%	C10 EW 13.1%
Treatment	none	1 nm–3 nm.	1 nm–3 nm
	air/350 °C	n.d.	1 nm–3 nm
	air/300 °C then H_2/350 °C	n.d.	17 nm
	H_2/350 °C	n.d.	18 nm
	H_2/350 °C then C_6H_6/H_2	23 nm	21 nm

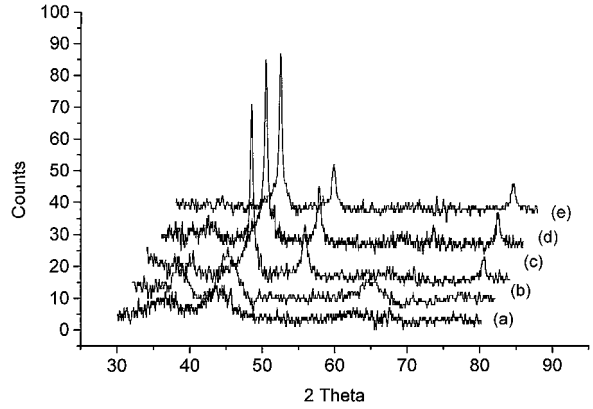

Figure 1 XRD spectra of the C10EW NiRCS catalyst (after subtraction of the spectrum of the support): (a) untreated; (b) treated under air/300 °C; (c) treated under air/300 °C then H_2/350 °C; (d) treated under H_2/350 °C; (e) used in the gas phase hydrogenation of benzene.

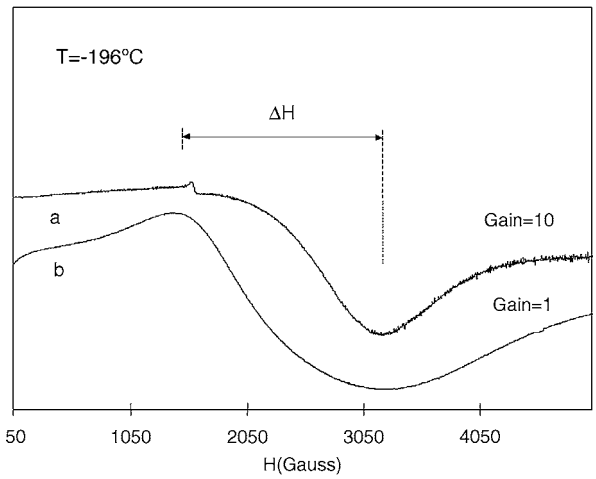

Figure 2 EPR spectra of C11EW recorded at −196°C: (a) before and (b) after the catalytic reaction.

was oxidized into the simple oxide NiO with characteristic 2θ bands at 37.2°, 43.3° and 62.9° (Fig. 1b). The metal particle size did not increase significantly during calcination (<5 nm). In contrast, it increased in the case of the thermal treatment under H_2 at 350°C (Fig. 1d), even when the sample was previously pretreated under air/300 °C (Fig. 1c) : particles as large as 17 nm–18 nm in diameter are obtained in these conditions (Table I). Particle size growth (up to about 21 nm–25 nm) also occurs during the reaction test (Fig. 2e, Table I).

It is worth noting that small particles were still present in the catalysts after the reductive thermal treatment or the reaction test. Indeed, close inspection of the XRD spectra (Fig. 1), shows an enlargement of the XRD signal at the foot of the band at $2\theta = 44.5°$. This large signal may be ascribed to smaller particles (<5 nm) not coalesced. One may speculate that such particles are in strong interaction with the support which then plays the role of a stabilizing matrix. In other words, the nickel phase would be preserved from sintering when it is in close contact with the support, probably on specific sites. In this way it is interesting to report the modeling study of Ni_6 nickel clusters (one or two layers) supported on alumina [27] : using CO as a probe molecule, the theoritical calculations showed a strong interaction

between the nickel atoms and support for the first but not the second layer. Further investigations are needed to understand the nickel phase stability as a function of the metal content in the case of reduced particles deposited on alumina.

4. EPR Spectroscopy

Figs 2 and 3 show the EPR spectra recorded at −196°C and 20°C of NiRC/alumina before and after the catalytic test. All the spectra obtained manifest broad signals. Generally, the g factor and the peak-to-peak linewidth (ΔH_{pp}) values depend on the temperature and the nickel content (Table II). Similar signals were obtained in organometallic compounds [28, 29] and quartz [30] and were attributed to Ni^+ species (d^9). The presence of Ni^+ ions in NiRC/alumina can be due to an incomplete reduction of a nickel acetate (Ni^{2+} is in the low spin state: $S = 0$) used as precursor during the preparation step. Indeed, blank experiments showed that the alumina support and the nickel acetate solid precursor did not give EPR signals whereas the NiRC prepared gave one which was similar to that obtained on NiRCS (Table II). Therefore, the environmental symmetry of Ni^+ ions ought be similar to that corresponding to Ni^0, the expected species in the catalyst. Consequently, the first species would be an indicator of the presence and size of Ni^0 entities in the solid.

TABLE II EPR Parameter values (X-band) of spectra obtained on Ni-precursor, support, NiRC, NiRCS (fresh and used samples)

Sample	g ($T = 20\,°C$)	ΔH (G) ($T = 20\,°C$)	ΔH (G) ($T = -196\,°C$)
Al_2O_3	—	—	—
$Ni(OAc)_2$	—	—	—
NiRC (11.7%)*	2.204	690	2630
NiRCS (5.4%) unwashed, untreated	2.236	910	1580
NiRCS (7.6%) washed, untreated	2.24	824	2500
NiRCS H_2/350°C then C_6H_6/H_2	2.33	1360	2259

*nickel composition of the catalyst.

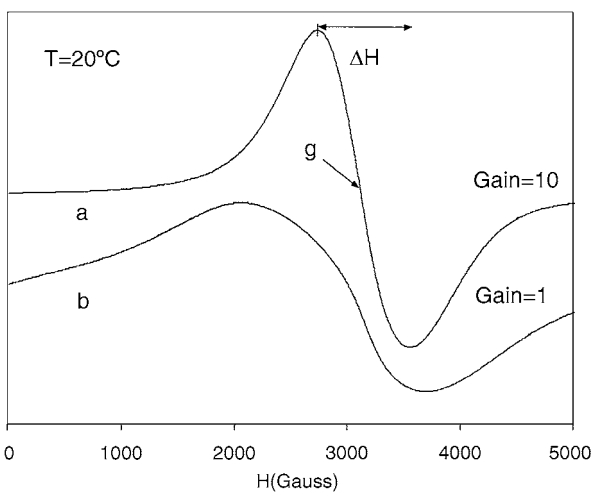

Figure 3 EPR spectra of C11EW recorded at 20°C: (a) before and (b) after the catalytic reaction.

Before the catalytic test (Fig. 2), the EPR signal of NiRC/alumina is centered at $g = 2.24$ with $\Delta H_{pp} = 824$ G and $\Delta H_{pp} = 2500$ G when the sample is recorded at 25 °C and −196 °C respectively. The increase in the linewidth when the temperature decreased can be explained by the fact that the Ni^+ species are present in the alumina support in the form of agglomerates and not isolated and/or cluster forms. In order to confirm this hypothesis, the sample was recorded in the EPR spectrometer at −196°C with a Q-band frequency (35 GHz) instead of an X-band frequency (9.5 GHz). Since the linewidth increased from 2500 to 3300 G with the higher frequency, this means that the Ni^+ species are in the form of agglomerates and not isolated. Isolated paramagnetic species generally give signals with a decrease in the linewidth [31, 32].

Fig. 3 shows the EPR spectra of NiRCS obtained after the catalytic reaction. The intensity of the Ni^+ signal was drastically increased particularly that recorded for the catalyst previously treated under hydrogen. In addition the signals were broader and this phenomenon can be due to ferromagnetic properties of the nickel phase formed. The increase in the Ni^+ ion concentration and therefore in the Ni° species, can be explained by the partial decomposition of the organic matrix (see below). These results are in agreement with the present X-ray diffraction results and previous electron microscopy studies [25].

5. TGA experiments

The thermograms involved two main domains, one at low temperature, around 100°C and the other at a higher temperature in the range of 200°C–400°C. In the latter domain, the shape and temperature of the peaks both changed as a function of the nickel loading as illustrated in Fig. 4 in the case of the C8EW (4.3% Ni) and C10EW (13.1% Ni) catalysts. The former exhibits a narrow peak at 380 °C wheras the latter is composed of a broad peak at 340 °C and a shoulder around 380 °C.

The first domain of the thermogram is attributed to the desorption of physisorbed water and/or tBuOH [25]. The presence of physisorbed H_2O molecules was due to exposure of the samples to atmospheric moisture during

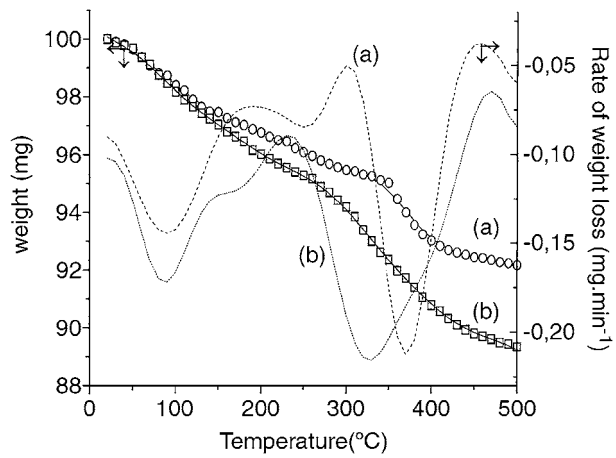

Figure 4 TGA profiles under N_2 for the (a) C8EW (4.3% Ni) and (b) C10EW (13.1% Ni) catalysts.

handling. As to that of the tBuOH molecules it probably resulted from the interaction of atmospheric moisture with the residual strong base tBuONa component of the NiRCS complex [25]. The high temperature peaks (200 °C–400 °C) are due to the decomposition of two or more carbonaceous species interacting with the solid surface with a strength depending on the nickel content.

On the other hand, the XRD (Table I, Fig. 1) and EPR experiments (Table II, Figs 2 and 3) clearly show an increase of the particle size after thermal treatment under H_2 or after $C_6H_6 + H_2$ reaction but almost not under air. It can be conjectured that the particle size growth is related to the thermal decomposition of the organic matrix in reductive but not oxidative conditions. Indeed, under reductive atmosphere, surface diffusion and coalescence of the bare metal nickel particles occurred. Such a mechanism probably holds for those particles not in interaction with the support. These particles exhibit the characteristic XRD band at $2\theta = 44.5°$ (Fig. 1). In contrast, for the fraction of particles in stronger interaction with alumina a stabilizing effect of the support is expected and no size growth can be observed (see above). They give rise to the enlargement of the XRD signal at the foot of the Ni° characteristic band (Fig. 1). In contrast, in oxidative conditions, the decomposition of the organic matrix led to more stable nickel oxide particles. In addition, these oxide particles were probably attached to the support by strong Ni^{2+}- O bonds, and thus less prone to sintering.

6. Catalytic activity in the hydrogenation reaction of benzene

6.1. Stability of the NiRCS materials under the reaction conditions

The catalysts were pre-treated under H_2 flow at 350 °C before testing in order to remove the organic fragment still remaining on the surface (see TGA results) and which inhibited the reaction [25]. All catalysts were 100% selective to cyclohexane. Steady-state activity was rapidly reached and the catalysts remained stable with time on stream for several hours (up to about 30 h) as illustrated in Fig. 5 for the C10EW catalyst. The figure shows that, indeed, a quasi-stable activity is obtained at each reaction temperature. In addition, the catalyst can be regenerated by a thermal treatment under H_2: the activity is then almost totally recovered (Fig. 6).

6.2. Effect of the reaction conditions

The catalysts exhibited a maximum of conversion as a function of the reaction temperature, notably at low nickel content (Fig. 6), in good agreement with the literature data [33–40]. The maximum of activity with temperature is attribuable to the competitive adsorption of the benzene and H_2 reactant molecules [33–40]. At a low reaction temperature, the benzene molecule should be strongly adsorbed on the nickel phase and thus inhibit the adsorption of the H_2 molecule; consequently, the catalytic activity is low. At a higher reaction temperature the adsorption of the reactant molecules is lower and the hydrogenation activity of the catalyst is also

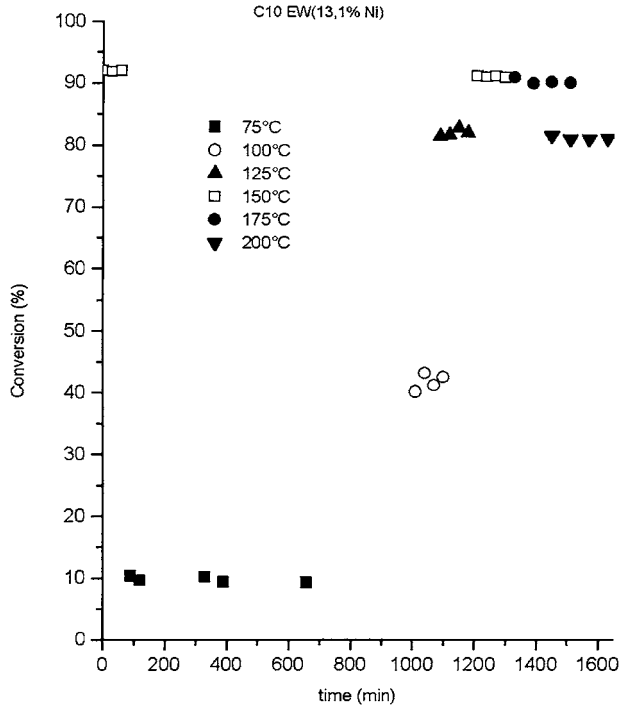

Figure 5 Benzene hydrogenation over the C10EW catalyst. Variation of the conversion as a function of time on stream. Flow rate = 50 mL · min^{-1}; $P_{C6H6}/P_{H2} = 0.05$; $m = 150$ mg.

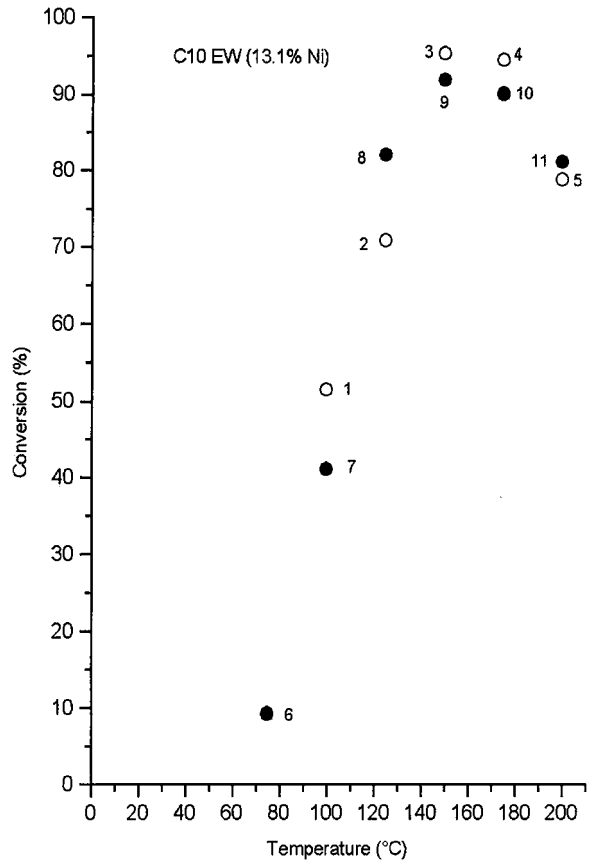

Figure 6 Regeneration of the NiRCS catalysts used in benzene hydrogenation. Procedure: (i) increase of the reaction temperature from 100 °C (point 1) to 200 °C (point 5); (ii) treatment under H2/350 °C/2 h; (iii) cooling down to 75 °C; (d) increase of the reaction temperature from 75 °C (point 6) to 200 °C (point 11). Variation of the conversion as a function of time on stream and reaction temperature. Flow rate = 50 mL · min^{-1}; $P_{C6H6}/P_{H2} = 0.05$; $m = 150$ mg.

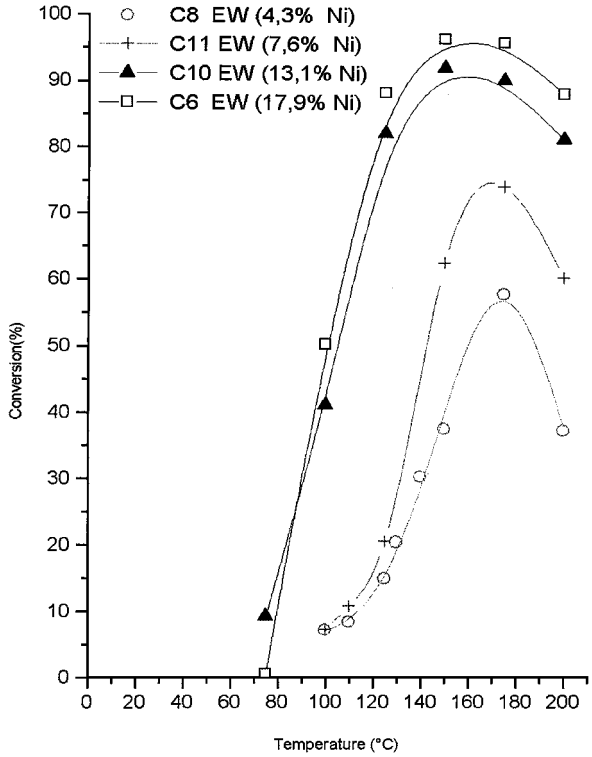

Figure 7 Benzene hydrogenation over the NiRCS catalysts. Conversion as a function of the nickel composition and reaction temperature. Flow rate = 50 mL · min^{-1}; $P_{C6H6}/P_{H2} = 0.05$; $m = 150$ mg.

TABLE III Effect of the C_6H_6/H_2 ratio on the conversion of benzene. Temperature = 100°C; Flow rate = 50 mL · min^{-1}; $m = 150$ mg

C_6H_6/H_2 ratio	Benzene conversion %
0.05	45.5
0.06	43.0
0.07	38.0
0.09	34.0

low. At medium temperatures a maximum of activity is observed (Fig. 7).

The study of the relative partial pressure of the reactants on the conversion confirmed the role of adsorption phenomena in the determination of the activity of the catalysts. The results obtained showed that the conversion decreased from 45.5% to 35% as the C_6H_6/H_2 ratio was increased from 0.050 to 0.085 (Table III). Thus, the higher the benzene partial pressure the lower the conversion. This is the consequence of the greater extent of the aromatic molecule adsorption on the catalyst surface at the expense of that of the H_2 molecule, in good accordance with published kinetic studies [35, 36].

6.3. Effect of the nickel loading

Conversion of benzene increased with the nickel loading as shown in Fig. 7. At 150 °C for example, the conversion increased from 25% to 90% when the nickel composition increased from 4.3% Ni to 17.9% Ni. The increase of activity is related to the increase of the concentration of the surface metal active sites with the nickel content. Another effect of the nickel composition on the reaction is the change in the temperature of the maximum of benzene conversion (Fig. 7). For low nickel compositions (4.3% and 7.6%) a definite maximum is observed around 175°C. At higher nickel loading, the conversion reached a flat maximum around 150 °C. The shift of the maximum in the lower range of the reaction temperature clearly indicates that the activity of the nickel phase increased with the nickel loading. Changes in the strucure of the active site have probably been induced by the increase of the nickel composition. Further investigation are needed for a better understanding of these changes.

7. Conclusions

In the present paper we report the results obtained on the structure and stability of nanoparticles of metallic nickel inserted in an organic matrix and supported on alumina. XRD and EPR studies confirmed the nanometric size of the fresh particles. Part of the organic matrix remained on the final material and two or more organic species according to the nickel composition were shown by the TGA technique. The size of the particles increased (up to about 20 nm) after thermal treatment under H_2 flow at 350 °C or during benzene hydrogenation but not after thermal treatment under air flow at 300 °C. TGA and reaction test experiments suggested that the metal particle coalescence was related to the thermal decomposition of the organic matrix. In contrast, thermal treatment under air flow rather induced stable nickel oxide particles, firmly bonded to the support and less prone to growth. The catalysts pre-treated under H_2/350 °C exhibited good activity and stability in the benzene hydrogenation reaction in the temperature range of 75 °C–200 °C. The activity depended on the reaction conditions and increased with the nickel composition. To sum up, the thermal stability or catalytic activity in gas phase media of the studied metallic nickel particles deposited on an alumina support depends on both the chemical nature of the treatment atmosphere and the nickel phase content.

References

1. G. SCHMIDT, *Chem. Rev.* **92** (1992) 1709.
2. H. GLEITER, *Nanostruct. Mater.* **1** (1992) 1.
3. R. P. ANDRES, J. D. BIEFIELD, J. I. HENDERSON, D. B. JANES, V. R. KOLAKUNDA, C. P. KUBIAC, W. J. MAHONEY and R. G. OSIFCHIN, *Science* **273** (1996) 1690.
4. C. SURYANARYANA, D. MUKHOPADHYAY, N. PAVILAKARS and F. H. FROESS, *J. Mater. Res.* **7** (1992) 8.
5. S. DAVIS and K. J. KLABUNDE, *Chem. Rev.* **82** (1982) 153.
6. M. JOSE-YACAM and R. F. MEHL, *Metall. Mater. Trans.* **29** (1998) 713.
7. H. WELLER, *Angew. Chem., (Int. Ed. Engl.)* **35** (1996) 1079.
8. C. ESTOURNES, T. LUTZ, J. HAPPISCH, T. QUARABTA, P. WISSLER and J. L. GUILLE, *J. Magn. Mater.* **173** (1997) 83.
9. H. VAN SWYGENHOVEN and A. CARO, *Nanostruct. Mater.* **9** (1997) 669.
10. L. K. KURIHARA, G. M. CHOW and P. E. SHOEN, *ibid.* **5** (1995) 607.
11. T. D. XIAO, S. TORBAN, P. R. STRUT and B. H. KEAR, *ibid.* **7** (1996) 857.
12. J. H. FENDLER and F. C. MELDRUM, *Adv. Mater.* **7** (1991) 607.

13. F. FIEVET, F. FIEVET-VINCENT, J. P. LAGIER, B. DUMONT and M. FILGARZ, *J. Mater. Chem.* **3** (1993) 627.
14. R. D. RIEKE, *Acc. Chem. Res.* **10** (1997) 377.
15. *Idem.*, *Science* **246** (1989) 1260.
16. G. A. OZIN, *Adv. Mater.* **4** (1992) 612.
17. G. N. GLAVEE, *Inorg. Chem.* **32** (1993) 474.
18. H. BONNEMAIN, W. BRIJOUX and T. JOUSSEN, *Angew. Chem. (Int. Ed. Engl.)* **29** (1990) 273.
19. D. ZENG and M. J. HAMPTEN-SMITH, *Chem. Mater.* **5** (1993) 68.
20. K. VIJAYA SARATHY, G. U. KULKARNY and C. N. R. RAO, *Chem. Commun.* (1997) 537.
21. P. GALLEZOT, C. LECLERCQ, Y. FORT and P. CAUBERE, *J. Mol. Cat.* **93** (1994) 79.
22. J. J. BRUNET, D. BESOZI, A. COURTOIS and P. CAUBERE, *J. Amer. Chem. Soc.* **104** (1982) 7130.
23. J. J. BRUNET, P. GALLOIS and P. CAUBERE, *J. Org. Chem.* **45** (1980) 1937.
24. *Idem.*, *ibid.* **45** (1980) 1946.
25. D. FRANQUIN, S. MONTEVERDI, S. MOLINA, M. M. BETTAHAR and Y. FORT, *J. Mater. Sci.* **34** (1999) 1.
26. S. ILLY, O. TILLEMENT, J. M. DUBOIS, Y. FORT and J. GHANBAJA, *Phil. Mag. A* **79** (1999) 1021.
27. G. PACCHIONI and N. RÖSCH, *Surf. Sci.* **306** (1994) 169.
28. H. C. LONGUETT-HIGGINS and A. J. STONES, *Mol. Phys.* **5** (1962) 417.
29. H. A. KUSKA and M. T. RODGERS, in "Electron Spin Resonance of First Row Transition Metal Complex Ions," edited by E. T. Kaiser and L. Kevan (Interscience Publishers, John Wiley and Sons, New York, London, Sidney, 1968).
30. F. W. LYTLE and R. B. GREEKOR, *Mat. Res. Soc. Symp. Proc.* **61** (1986) 259.
31. S. ANGELOV, C. FRIEBEL, E. ZHECHEVA and R. STYANOVA, *J. Phys. Chem. Solids* **53** (1992) 443.
32. D. GOLDFARB, M. BERNARDO, K. G. STROHMAIER, D. E. W. VAUGHAN and H. THOMANN, *J. Am. Chem. Soc.* **116** (1994) 6344.
33. G. A. MARTIN and J. A. DALMON, *J. Catal.* **75** (1982) 233.
34. R. C. Z. VAN MEERTEN and J. W. E. COONEN, *ibid.* **37** (1975) 37.
35. S. SMETS, T. SALMI and D. MURZIN, *Appl. Catal. A* **145** (1996) 253.
36. M. A. KEANE, *J. Catal.* **166** (1997) 347.
37. C. MIRODATOS, J. A. DALMON and G. A. MARTIN, *ibid.* **105** (1987) 405.
38. J. W. E. COONEN, R. C. Z. VAN MEERTEN and H. T. RIJNTEN, in Proc. 5th Intern. Congr. Catal., Florida, 1972, edited by J. W. Hightoower (North-Holland, Amsterdam) p. 671.
39. P. N. RYLANDER, "Hydrogenation Methods" (Academic Press, 1985).
40. L. CERVENY, in "Catalytic Hydrogenation," Vol. 27 (Elsevier, Amsterdam, 1986).

Received 19 July
and accepted 20 December 2000